AD NUMBER

ADB005079

LIMITATION CHANGES

TO:

Approved for public release; distribution is unlimited.

FROM:

Distribution authorized to U.S. Gov't. agencies only; Test and Evaluation; JUN 1975. Other requests shall be referred to Army Ballistic Research Laboratory, Attn: AMXBR-SS, Aberdeen Proving Ground, MD 21005.

AUTHORITY

usaaradcom ltr, 20 feb 1981

BRL

MEMORANDUM REPORT NO. 2494

STABILITY OF SUBHARMONIC LIMIT MOTIONS OF A SLIGHTLY ASYMMETRIC MISSILE

C. Murphy
B. A. Hodes
J. W. Bradley

June 1975

USA BALLISTIC RESEARCH LABORATORIES
ABERDEEN PROVING GROUND, MARYLAND

Destroy this report when it is no longer needed.
Do not return it to the originator.

Secondary distribution of this report by originating or sponsoring activity is prohibited.

Additional copies of this report may be obtained from the Defense Documentation Center, Cameron Station, Alexandria, Virginia 22314.

The findings in this report are not to be construed as an official Department of the Army position, unless so designated by other authorized documents.

UNCLASSIFIED

SECURITY CLASSIFICATION OF THIS PAGE (When Data Entered)

REPORT DOCUMENTATION PAGE

READ INSTRUCTIONS BEFORE COMPLETING FORM

1. REPORT NUMBER: BRL Memorandum Report No. 2494	2. GOVT ACCESSION NO.
3. RECIPIENT'S CATALOG NUMBER	
4. TITLE (and Subtitle): STABILITY OF SUBHARMONIC LIMIT MOTIONS OF A SLIGHTLY ASYMMETRIC MISSILE	5. TYPE OF REPORT & PERIOD COVERED: Final
	6. PERFORMING ORG. REPORT NUMBER
7. AUTHOR(s): C. H. Murphy, B. A. Hodes, J. W. Bradley	8. CONTRACT OR GRANT NUMBER(s)
9. PERFORMING ORGANIZATION NAME AND ADDRESS: U. S. Army Ballistic Research Laboratories, Aberdeen Proving Ground, Maryland 21005	10. PROGRAM ELEMENT, PROJECT, TASK AREA & WORK UNIT NUMBERS: RDT&E 1T161102A33H
11. CONTROLLING OFFICE NAME AND ADDRESS: US Army Materiel Command, 5001 Eisenhower Avenue, Alexandria, VA 22333	12. REPORT DATE: JUNE 1975
	13. NUMBER OF PAGES: 45
14. MONITORING AGENCY NAME & ADDRESS (if different from Controlling Office)	15. SECURITY CLASS. (of this report): UNCLASSIFIED
	15a. DECLASSIFICATION/DOWNGRADING SCHEDULE

16. DISTRIBUTION STATEMENT (of this Report)

Distribution limited to US Government agencies only; Test and Evaluation; June 1975. Other requests for this document must be referred to Director, USA Ballistic Research Laboratories, ATTN: AMXBR-SS, Aberdeen Proving Ground, MD 21005

17. DISTRIBUTION STATEMENT (of the abstract entered in Block 20, if different from Report)

18. SUPPLEMENTARY NOTES

19. KEY WORDS (Continue on reverse side if necessary and identify by block number)

Stability Analysis
System Stability
Subharmonic Limit Motion
Asymmetric Missile
Cubic Static Moment
Routh-Hurwitz Stability Criterion
Perturbation Analysis
Quasi-Linear Analysis

20. ABSTRACT (Continue on reverse side if necessary and identify by block number) (jah)

A cubic static moment acting on a slightly asymmetric missile can (under certain conditions) produce a nonharmonic steady-state response. For small amplitude motion, this response occurs at one-third the spin rate and hence is called a subharmonic response. The equations defining the conditions under which a nonharmonic response will occur impose an upper bound on the non-negative damping parameter $\hat{H}$. For a given $\hat{H}$ less than this upper bound, there are two possible nonharmonic motions. In this report we show that one of these

DD FORM 1 JAN 73 1473 EDITION OF 1 NOV 65 IS OBSOLETE

UNCLASSIFIED

SECURITY CLASSIFICATION OF THIS PAGE (When Data Entered)

BLOCK 20 (Abstract)(continued):

motions is stable, the other unstable; that is, the stability/instability boundary occurs where $\hat{H}$ is at its upper limit. A simple approximate relation is presented for establishing whether a given set of parameters will produce a stable or unstable nonharmonic steady-state response.

TABLE OF CONTENTS

LIST OF ILLUSTRATIONS

LIST OF TABLES

I. INTRODUCTION

The usual effect of a slight asymmetry, caused, say, by an offset center of gravity or a bent fin, is to add a constant moment that rolls with the missile to the total aerodynamic moment acting on the missile.[1] The response to this asymmetry moment is a trim angle that also rolls with the missile. The magnitude of this trim angle is a function of the spin rate: this magnitude grows from its value for zero spin, δ_{T0}, to a maximum resonance value, δ_{TR}, reached when the spin rate equals the pitch rate, and then decays to zero as the spin increases further.

We have already studied the effect of a cubic static moment on the motion of a slightly asymmetric missile, using a general quasi-linear averaging technique.[2] Except under certain special spin conditions, the effect is to change the frequencies of the transitory modes of oscillation and the magnitude of the steady-state trim angle. For a dynamically stable missile, the transitory modes damp out and only the harmonic response to the asymmetry forcing function remains.

Recently, however, we have shown that under certain conditions a nonharmonic steady-state response is possible.[3-4] We call this nonharmonic response a generalized subharmonic response because for small amplitude motion it occurs at one-third the spin rate. Although the theory of Reference 3 predicted two possible nonharmonic motions, we have been able to generate only one of these by numerical integration. We conjectured that the other motion is unstable and it is the purpose of this memorandum report to prove this conjecture.

---

1. *John D. Nicolaides, "On the Free Flight Motion of a Missile with Slight Configurational Asymmetries," Ballistic Research Laboratories Report No. 858, AD 26405, June 1953; also IAS Preprint 395, January 1953.*

2. *Charles H. Murphy, "Nonlinear Motion of a Missile with Slight Configurational Asymmetries," J. Spacecraft and Rockets, Vol. 8, March 1971, pp. 259-263; also Ballistic Research Laboratories Memorandum Report No. 2036, AD 870704, May 1970.*

3. *Charles H. Murphy, "Generalized Subharmonic Response of a Missile with Slight Configurational Asymmetries," Ballistic Research Laboratories Report No. 1591, AD 749787, June 1972; also AIAA Paper 72-972, September 1972.*

4. *Charles H. Murphy, "Subharmonic Behavior of a Slightly Asymmetric Missile," AIAA Journal, Vol. 11, June 1973, pp. 884-885.*

II. NONLINEAR ANALYSIS

If we limit the nonlinearity under consideration to a cubic static moment and neglect any linear Magnus moment contribution, the transverse moment expansion assumes the form

$$C_{\tilde{m}} + i\, C_{\tilde{n}} = -\, i \left[C_{M_0}\, e^{i\phi} + (c_0 + c_2\delta^2)\tilde{\xi} + C_{M_{\dot{\alpha}}}\, \tilde{\xi}' \right] + C_{M_q}\, \tilde{\mu} \qquad (1)$$

For zero spin and linear static moment ($c_2 = 0$), this moment expansion induces a trim angle of δ_{T0} . The ratio m_a of the cubic part of the static moment to the linear part for this trim angle is a most important parameter. It is a measure of both the size of the asymmetry and the size of the nonlinearity. By use of this parameter, the nonlinear differential equation for the angular motion induced by the aerodynamic moment of Equation (1) can be written as[3]

$$\tilde{\xi}'' + (H - iP)\tilde{\xi}' - M_0\, [1 + m_a\, (\delta/\delta_{T0})^2]\tilde{\xi} = -\, M_0 \delta_{T0} e^{i\phi} \qquad (2)$$

Equation (2) and various relations involving its solution can be considerably simplified by a change of the independent variable from s to τ, where $\tau = (-M_0)^{\frac{1}{2}}\, s$. If we use dots to denote derivatives with respect to τ, Equation (2) becomes

$$\ddot{\tilde{\xi}} + (\hat{H} - i\hat{P})\dot{\tilde{\xi}} + [1 + m_a\, (\delta/\delta_{T_0})^2]\tilde{\xi} = \delta_{T0} e^{i\phi} \qquad (3)$$

where $\hat{(\ )} = (\ )\ (-M_0)^{-\frac{1}{2}}$

The linear angular motion of a slightly asymmetric missile ($m_a = 0$) is described by the usual tricyclic equation[1]

$$\tilde{\xi} = \delta_{T0} \left[k_1\, e^{i\phi_1} + k_2\, e^{i\phi_2} + k_3\, e^{i(\phi + \phi_{30})} \right] \qquad (4)$$

Relations for the parameters ($\dot{\phi}_1$, $\dot{\phi}_2$, k_1 , k_2 , k_3, ϕ_{30}) of Equation (4) can be obtained by an averaging process.[2] If $\dot{\phi}$ is not near zero or unity, these relations take the form:[3]

$$\dot{\phi}_j\ (\dot{\phi}_j - \hat{P}) = 1 + m_a\, (\delta_{ej}/\delta_{T0})^2 \qquad j = 1,\ 2 \qquad (5)$$

$$\dot{k}_1/k_1 = \hat{\lambda}_1 = -\left[\hat{H}\,\dot{\phi}_1 + \ddot{\phi}_1 - 2\,m_a\,k_2k_3\,(\sin\Psi)_{av}\right][2\dot{\phi}_1 - \hat{P}]^{-1} \tag{6}$$

$$\dot{k}_2/k_2 = \hat{\lambda}_2 = -\left[\hat{H}\dot{\phi}_2 + \ddot{\phi}_2 + m_a\,k_1^2k_3k_2^{-1}\,(\sin\Psi)_{av}\right][2\dot{\phi}_2 - \hat{P}]^{-1} \tag{7}$$

$$\Psi = 2\phi_1 - \phi_2 - \phi - \phi_{30} \tag{8}$$

$$k_3\left[1 - (1 - I_x/I_y)\dot{\phi}^2 + m_a(2k_1^2 + 2k_2^2 + k_3^2)\right] = \cos\phi_{30} - m_a k_1^2 k_2 (\cos\Psi)_{av} \tag{9}$$

$$-k_3\hat{H}\dot{\phi} = \sin\phi_{30} + m_a k_1^2 k_2 (\sin\Psi)_{av} \tag{10}$$

where

$$\left(\delta_{e_1}/\delta_{T0}\right)^2 = k_1^2 + 2k_2^2 + 2k_3^2 + 2k_2k_3(\cos\Psi)_{av}$$

$$\left(\delta_{e_2}/\delta_{T0}\right)^2 = k_2^2 + 2k_1^2 + 2k_3^2 + k_1^2k_3k_2^{-1}\,(\cos\Psi)_{av}$$

In Reference 3 we showed that nonharmonic steady-state solutions can exist when Ψ is constant. The precise conditions for these solutions are:

$$\dot{\Psi} = 0 \tag{11a}$$

$$\hat{\lambda}_1 = \hat{\lambda}_2 = 0 \tag{11b}$$

The values of $(k_1, k_2, k_3, \phi_{30}, \Psi)$ associated with a steady-state solution will be identified by bar superscripts. Conditions (11) give a simple relation between $\bar{k}_1$ and $\bar{k}_2$ and a more involved relation between $\bar{\Psi}$ and $\hat{H}$:

$$\bar{k}_1^2 = 2b\ \bar{k}_2^2 \tag{12}$$

$$\sin\bar{\Psi} = \hat{H}\dot{\bar{\phi}}_1\ (2m_a\bar{k}_2\bar{k}_3)^{-1} \tag{13}$$

where

$$b = -\ \dot{\bar{\phi}}_2/\dot{\bar{\phi}}_1 \cong 1$$

Equations (9, 10, 11a, 12, 13) constitute five equations for the five unknown parameters ($\bar{k}_1$, $\bar{k}_2$, $\bar{k}_3$, $\bar{\phi}_{30}$, $\bar{\Psi}$). For the algebraically simpler case where $I_x/I_y << 1$, a concise form of these equations is given in Table 1 .

TABLE 1. CONDITIONS FOR STEADY-STATE NONHARMONIC SOLUTION WHEN $I_x/I_y << 1$

$$\bar{k}_1^2 = 2b\ \bar{k}_2^2 \tag{T1:1}$$

$$\sin\bar{\Psi} = \hat{H}\dot{\phi}[2(2+b)m_a\bar{k}_2\bar{k}_3]^{-1} \tag{T1:2}$$

$$1 + m_a[2(b+1)\bar{k}_2^2 + 2\bar{k}_3^2 + 2\bar{k}_2\bar{k}_3\cos\bar{\Psi}] = [\dot{\phi}/(2+b)]^2 \tag{T1:3}$$

$$\bar{k}_3\left\{1 - \dot{\phi}^2 + m_a[2(2b+1)\bar{k}_2^2 + \bar{k}_3^2]\right\} = \cos\bar{\phi}_{30} - 2m_a b\bar{k}_2^3\cos\bar{\Psi} \tag{T1:4}$$

$$\sin\bar{\phi}_{30} = -\hat{H}\dot{\phi}[\bar{k}_3^2 + (b/2+b)\bar{k}_2^2]k_3^{-1} \tag{T1:5}$$

$$\dot{\bar{\phi}}_1 = \left\{1 + m_a[2(b+1)\bar{k}_2^2 + 2\bar{k}_3^2 + 2\bar{k}_2\bar{k}_3\cos\bar{\Psi}]\right\}^{1/2} \tag{T1:6}$$

$$\dot{\bar{\phi}}_2 = -\left\{1 + m_a\ [(4b+1)\bar{k}_2^2 + 2\bar{k}_3^2 + 2b\bar{k}_2\bar{k}_3\cos\Psi]\right\}^{1/2} \tag{T1:7}$$

$$b = -\frac{\dot{\bar{\phi}}_2}{\dot{\bar{\phi}}_1} \tag{T1:8}$$

The relations in this table can be solved by an iterative process for a given m_a, $\dot{\phi}$ and $\hat{H}$, provided that $\dot{\phi}$ and $\hat{H}$ satisfy certain restrictions. Equation (T1:3) requires $\dot{\phi} > 3$ (that is, the spin must exceed three times the resonance spin) when m_a is positive and $\dot{\phi} < 3$ when m_a is negative. Equation (T1:2) imposes an upper bound on $\hat{H}$: this bound is shown in Figure 1 for $m_a = \pm 0.2$.

For each $\hat{H}$ less than this upper bound, the relations in Table 1 yield two solutions, identified in Figures 2-5 by solid and dashed lines. Figures 2 and 3 are plots of $\bar{k}_2$ and $\bar{k}_3$, respectively, versus spin for zero $\hat{H}$ and various m_a values. Figures 4 and 5 are plots of $\bar{\phi}_{30}$ and $\bar{\Psi}$, respectively, versus $\hat{H}$ for $m_a = 0.2$ and various spins.

The solutions identified by dashed lines in Figures 2-5 are the ones that have not been obtained by direct numerical integration and the ones that we want to show are unstable.

III. SOLUTION FOR $\bar{k}_3 = 0$

As we can see from Figure 3, $\bar{k}_3$ passes through zero for one set of solutions. The nature of the solution is different above and below the critical value of $\dot{\phi}$, say $\dot{\phi}_c$, at which $\bar{k}_3 = 0$. Thus it is of some interest to derive a set of equations for determining $\dot{\phi}_c$ for a given m_a .

From Equations (T1:2) and (T1:5), we have

$$\sin \bar{\phi}_{30} = - 2m_a \bar{k}_2 \left[b\, \bar{k}_2^2 + (2+b)\bar{k}_3^2 \right] \sin\bar{\Psi} \qquad (14)$$

When $\bar{k}_3 = 0$, Equations (14) and (T1:4) reduce to

$$\sin\bar{\phi}_{30} = - (2m_a b\bar{k}_2^3)\sin\bar{\Psi} \qquad (15)$$

$$\cos\bar{\phi}_{30} = (2m_a b\bar{k}_2^3)\cos\bar{\Psi} \qquad (16)$$

Thus we must have

$$2m_a b\, \bar{k}_2^3 = \pm 1 , \quad \bar{k}_3 = 0 \qquad (17)$$

Next, we note that for $\bar{k}_3 = 0$, Equations (T1:6-T1:8) reduce to

$$\bar{\phi}_1^2 = 1 + 2(b + 1)m_a\bar{k}_2^2 \tag{18}$$

$$\bar{\phi}_2^2 = 1 + (4b + 1)m_a\bar{k}_2^2 \tag{19}$$

$$b^2 = \frac{1 + (4b + 1)m_a\bar{k}_2^2}{1 + 2(b + 1)m_a\bar{k}_2^2} \tag{20}$$

Solving Equation (20) for $m_a\bar{k}_2^2$, we have

$$m_a\bar{k}_2^2 = \frac{b^2 - 1}{D} \tag{21}$$

where

$$D = D(b) \equiv 1 + 4b - 2b^2(1 + b) \tag{22}$$

Substituting Equation (21) in Equation (17), we obtain

$$m_a = \frac{4b^2(b^2 - 1)^3}{D^3} \tag{23}$$

For zero $\bar{k}_3$ and any m_a, we can solve Equation (23) for b, then use Equations (18) and (21) to obtain the critical value of $\dot{\phi}$:

$$\dot{\phi}_c = (2 + b)\bar{\phi}_1$$

$$= (2 + b)\left[1 + \frac{2(b+1)(b^2-1)}{D}\right]^{\frac{1}{2}} \tag{24}$$

Critical values for a range of m_a are listed in Table 2 (the approximation column is discussed in the next section). Note that - 1/27 is the minimum m_a for which $\bar{k}_3$ will go to zero. As m_a increases, b approaches $b_M \cong 1.14$, the only positive root of the cubic equation

$$D = 0 \tag{25}$$

It can be shown that whether or not $\bar{k}_3$ is zero, b_M is an upper bound on b .

TABLE 2. CRITICAL SPIN VALUES ($\bar{k}_3 = 0$)

m_a	b(Eq. 23)	$\bar{k}_2$	$\dot{\phi}_c$(Eq. 24)	APPROX $\dot{\phi}_c$(Eq. 43)
- 1/27	0.5	3.	0.	0.775
- .03	0.65505	2.94120	0.99684	1.082
- .01	0.86737	3.86298	1.90778	1.890
- .001	0.95931	8.04768	2.55635	2.546
0	1	∞	3.	3.
.001	1.02570	7.87014	3.38411	3.394
.01	1.04567	3.62960	3.77834	3.799
.1	1.07143	1.67110	4.51085	4.549
.2	1.07944	1.32306	4.82601	4.872
.5	1.08962	0.97180	5.32761	5.385
1.0	1.09679	0.76963	5.78028	5.848
2.0	1.10333	0.60965	6.30441	6.383
.	.	.	.	
.	.	.	.	
.	.	.	.	
∞	1.13973	0	∞	

Finally, we note that when $\bar{k}_3 = 0$, Equations (T1:2) and (T1:4) imply that

$$\hat{H} = 0 \tag{26}$$

and Equations (15-17) imply that

$$\bar{\phi}_{30} + \bar{\Psi} = \pi \ , \ m_a < 0$$
$$= 2\pi, \ m_a > 0 \tag{27}$$

IV. APPROXIMATE RELATIONS

As can be seen from Figures 2 and 3, $\bar{k}_3$ terms can usually be neglected in comparison with $\bar{k}_2$ terms, at least when $\dot{\phi}$ is greater than and not too close to 3. When $\bar{k}_3$ is neglected, b is given by Equation (20). We see from this equation that for a given m_a, as $\bar{k}_2$ goes to zero, b approaches unity and as $\bar{k}_2$ increases, b approaches the positive root of Equation (25), namely $b_M \cong 1.14$. Thus a good first approximation for b is 1.

From Equations (8) and (11a) we have

$$\bar{\dot{\phi}}_1 = \frac{\dot{\phi}}{2 + b} , \quad \bar{\dot{\phi}}_2 = - \frac{b\dot{\phi}}{2 + b} \tag{28}$$

Hence for $b \cong 1$, our first approximation of the frequencies is:

$$\bar{\dot{\phi}}_1 \cong - \bar{\dot{\phi}}_2 \cong \frac{\dot{\phi}}{3} \tag{29}$$

Then from Equations (18-19, 29), we have

$$\bar{\dot{\phi}}_1^2 \cong 1 + 4m_a\bar{k}_2^2 \cong \frac{\dot{\phi}^2}{9} \tag{30}$$

$$\bar{\dot{\phi}}_2^2 \cong 1 + 5m_a\bar{k}_2^2 \cong \frac{\dot{\phi}^2}{9} \tag{31}$$

Equations (30) and (31) yield two possible approximations:

$$m_a\bar{k}_2^2 \cong \frac{\dot{\phi}^2 - 9}{36} , \frac{\dot{\phi}^2 - 9}{45}$$

The average gives an excellent first approximation for $\bar{k}_2$:

$$m_a\bar{k}_2^2 \cong \frac{\dot{\phi}^2 - 9}{40} \tag{32}$$

Substituting this result in Equations (30-31) we have the improved frequency approximations:

$$\bar{\dot{\phi}}_1^2 \cong \frac{\dot{\phi}^2 + 1}{10} \tag{33}$$

$$\bar{\dot{\phi}}_2^2 \cong \frac{\dot{\phi}^2 - 1}{8} \tag{34}$$

from which we can obtain an improved approximation for b:

$$b \cong \left[\frac{5(\dot{\phi}^2 - 1)}{4(\dot{\phi}^2 + 1)}\right]^{\frac{1}{2}} = \left[1 + \frac{\dot{\phi}^2 - 9}{4(\dot{\phi}^2 + 1)}\right]^{\frac{1}{2}}$$

$$\cong 1 + \frac{\dot{\phi}^2 - 9}{8(\dot{\phi}^2 + 1)} = \frac{9\dot{\phi}^2 - 1}{8(\dot{\phi}^2 + 1)} \tag{35}$$

Simple approximations for $\bar{k}_3$, $\bar{\phi}_{30}$ and $\bar{\Psi}$ can now be obtained. First, we neglect $\bar{k}_3^2$ in Equations (T1:4) and (14) so that they become, respectively,

$$\bar{k}_3 \cong \frac{2m_a b\bar{k}_2^3 \cos\bar{\Psi} - \cos\bar{\phi}_{30}}{\dot{\phi}^2 - 1 - 2(2b+1)m_a\bar{k}_2^2} \tag{36}$$

and

$$\sin\bar{\phi}_{30} \cong - 2m_a b\bar{k}_2^3 \sin\Psi$$

$$= - |m_a|^{-\frac{1}{2}} f_1(\dot{\phi}) \sin\Psi \tag{37}$$

where

$$f_1(\dot{\phi}) = 2b(m_a\bar{k}_2^2)\,|m_a\bar{k}_2^2|^{\frac{1}{2}} \tag{38}$$

with b and $m_a\bar{k}_2^2$ given by Equations (35) and (32). Next, we substitute the approximation (36) for $\bar{k}_3$ in Equation (T1:2) to obtain, with the help of Equation (37):

$$\frac{\hat{H}\phi\left[\dot{\phi}^2 - 1 - 2(2b + 1)m_a\bar{k}_2^2\right]}{2\ (2 + b)m_a\bar{k}_2} \cong \left(2m_a b\bar{k}_2^3 \cos\bar{\Psi} - \cos\bar{\phi}_{30}\right)\sin\bar{\Psi}$$

$$\cong - \sin\bar{\phi}_{30}\cos\bar{\Psi} - \cos\bar{\phi}_{30}\sin\bar{\Psi}$$

$$= - \sin(\bar{\phi}_{30} + \bar{\Psi})$$

or

$$\hat{H} \cong - \hat{H}_A \sin(\bar{\phi}_{30} + \bar{\Psi}) \tag{39}$$

where

$$\hat{H}_A = \frac{2\ (2 + b)m_a\bar{k}_2}{\dot{\phi}\left[\dot{\phi}^2 - 1 - 2(2b + 1)m_a\bar{k}_2^2\right]} = \frac{m_a f_2(\dot{\phi})}{|m_a|^{\frac{1}{2}}} \tag{40}$$

$$f_2(\dot{\phi}) = \frac{2(2 + b)\left|m_a\bar{k}_2^2\right|^{\frac{1}{2}}}{\dot{\phi}\left[\dot{\phi}^2 - 1 - 2(2b + 1)m_a\bar{k}_2^2\right]} > 0 \tag{41}$$

and where b and $m_a\bar{k}_2^2$ are again given by Equations (35) and (32). Thus the elaborate damping curves of Figures 4 and 5 would be transformed into a family of near sine waves if $\hat{H}$ were plotted against $\bar{\phi}_{30} + \bar{\Psi}$.

Note that $\hat{H}_A$ has the sign of m_a. Hence approximation (39) predicts that when $\hat{H}$ is at its maximum value $\hat{H}_{MAX}$ ($\cong |\hat{H}_A|$), then

$$\bar{\phi}_{30} + \bar{\Psi} \cong \begin{cases} \pi/2, & m_a < 0 \\ 3\pi/2, & m_a > 0 \end{cases} \tag{42}$$

We will test the adequacy of this prediction in the next section.

The process of approximation can be summarized as follows. For a given m_a, $\dot{\phi}$ and $\hat{H}$:

1. compute b and $m_a \bar{k}_2^2$, Equations (35) and (32);

2. compute f_1, f_2, $\hat{H}_A$ and $\bar{\Psi} + \bar{\phi}_{30}$, Equations (38), (41), (40) and (39);

3. from f_1 and $\bar{\Psi} + \bar{\phi}_{30}$, compute $\bar{\phi}_{30}$ and $\bar{\Psi}$, Equation (37);

4. compute $\bar{k}_3$, Equation (36).

An approximation for the critical spin $\dot{\phi}_c$ can also be easily obtained. Using Equation (32) and setting b = 1, we can write Equation (17) as:

$$\frac{4}{m_a}\left(\frac{\dot{\phi}_c^2 - 9}{40}\right)^3 \cong 1$$

or

$$\dot{\phi}_c^2 \cong 9 + 40\left(\frac{m_a}{4}\right)^{1/3} \tag{43}$$

Critical spin values computed from Equation (43) are given in the final column of Table 2. Note that although Equation (43) can be applied to $m_a \geq -4(9/40)^3 \cong -.046$, the approximation is poor below $m_a = -.03$.

V. EXACT SOLUTION

In Figure 6, exact solutions of Equations (T1:1-5) are given in the form of $\bar{\phi}_{30}$ versus $\bar{\Psi}$ plots for $m_a = \pm 0.2$ and various values of $\dot{\phi}$.

Note the two families of curves for $m_a = 0.2$. For spins between 3 and the critical value of 4.826, $\bar{\Psi}$ grows from 0 to π while $\bar{\phi}_{30}$ grows from π to $(\bar{\phi}_{30})_{MAX} < 3\pi/2$ and then decreases back to π . The value of $(\bar{\phi}_{30})_{MAX}$ can be estimated by setting $\bar{\Psi} = \pi/2$ in Equation (37). For spins greater than the critical value, $\bar{\phi}_{30}$ grows from π to 2π while $\bar{\Psi}$ grows from 0 to $(\bar{\Psi})_{MAX} < \pi/2$ and then decreases back to 0 . The value of $(\bar{\Psi})_{MAX}$ can be estimated by setting $\bar{\phi}_{30} = 3\pi/2$ in Equation (37).

For $m_a = -0.2$, there is only one family since no critical spin value exists. The equations of Table 1 lose their validity as we approach resonance ($\dot{\phi} = 1$); hence, curves for spin values less than 2 are not shown.

When $\hat{H} = 0$ (and $\bar{k}_3 \neq 0$), Equations (T1:2) and (T1:5) reduce to

$$\sin\bar{\Psi} = \sin\bar{\phi}_{30} = 0 \tag{44}$$

For any value of $\dot{\phi}$ and m_a, the particular values of $(\bar{\Psi}, \bar{\phi}_{30})$ for the two possible zero-damping solutions are given in Table 3 .

TABLE 3. ZERO DAMPING POINTS

m_a	$\dot{\phi} - \dot{\phi}_c$	$(\bar{\Psi}, \bar{\phi}_{30})_{\hat{H}=0}$ Unstable	Stable
neg	neg	$(-\pi, 2\pi)$	$(-\pi, \pi)$
neg	pos	$(0, \pi)$	$(-\pi, \pi)$
pos	neg	$(0, \pi)$	(π, π)
pos	pos	$(0, \pi)$	$(0, 2\pi)$

The labeling of the points as stable or unstable is at this point in the report only a supposition. In Figure 6, of course, only the last three pairs in Table 3 occur.

As we move from $(0, \pi)$ along any curve $\dot{\phi}$ = constant in Figure 6, $\hat{H}$ increases until it reaches its maximum value approximately at the intersection of that curve with the line L_A:

$$L_A : \bar{\phi}_{30} + \bar{\Psi} = \begin{cases} \pi/2, & m_a < 0 \\ 3\pi/2, & m_a > 0 \end{cases} \tag{45}$$

That is (as we noted in the previous section), line L_A approximates the maximum damping locus

$$L_H : \hat{H} = \hat{H}_{MAX} \tag{46}$$

which is our conjectured stability/instability boundary. To see just how well L_A approximates L_H, we computed the exact values of

$$U \equiv (\bar{\phi}_{30} + \bar{\Psi})_{\hat{H} = \hat{H}_{MAX}} \tag{47}$$

for a variety of $\dot{\phi}$ and m_a values. Figure 7 plots the difference $U - 3\pi/2$ versus $\dot{\phi}$ for $m_a = 0.2$ and 0.5. It was found that for positive m_a, this difference is very nearly proportional to $\sqrt{m_a}$:

$$U - 3\pi/2 \cong \sqrt{m_a}\, F(\dot{\phi}) > 0 \tag{48}$$

Note from Figure 7 that the approximation $L_A \cong L_H$ worsens as we approach $\dot{\phi} = 3$; this is because our assumptions in deriving approximation (39)(in particular, that $\bar{k}_3$ could be neglected in several equations) are inadequate near $\dot{\phi} = 3$. However, for $\dot{\phi}$ greater than, say, five, L_A is an excellent approximation to our conjectured boundary.

VI. STABILITY ANALYSIS

In order to determine the stability of a nonharmonic steady-state motion identified by the parameters $(\bar{k}_1, \bar{k}_2, \bar{k}_3, \bar{\phi}_{30}, \bar{\Psi})$, we must consider the behavior of motions near such a limit motion. Therefore, we must derive the differential equations for small perturbation functions $\eta_j(\tau)$ defined by the equations

$$k_1 = \bar{k}_1 + \eta_1 \tag{49}$$

$$k_2 = \bar{k}_2 + \eta_2 \tag{50}$$

$$k_3 = \bar{k}_3 + \eta_3 \tag{51}$$

$$\phi_{30} = \bar{\phi}_{30} + \eta_4 \tag{52}$$

$$\Psi = \bar{\Psi} + \eta_5 \tag{53}$$

If Equations (49-53) are substituted in Equation (5), the frequency $\dot{\phi}_j$ $(j = 1, 2)$ can be expressed as the sum of the frequency $\bar{\dot{\phi}}_j$ for the limit motion $(\bar{k}_1, \bar{k}_2, \bar{k}_3, \bar{\phi}_{30}, \bar{\Psi})$ and a linear function ε_j of the perturbation variables:

$$\dot{\phi}_j = \bar{\dot{\phi}}_j + \varepsilon_j \qquad j = 1, 2 \tag{54}$$

where the $\varepsilon_j = \varepsilon_j(\eta_1, \eta_2, \eta_3, \eta_5)$ are given in Table 4 for $I_x/I_y \ll 1$.

Differential equations for η_1, η_2 and η_5 can now be obtained by substituting Equations (49-53) in Equations (6-8); these too are given in Table 4 .

TABLE 4. PERTURBATION EQUATIONS FOR $I_x/I_y \ll 1$

$$\varepsilon_1 = (m_a/\dot{\bar{\phi}}_1)\Big[\bar{k}_1\eta_1 + (2\bar{k}_2 + \bar{k}_3\cos\bar{\Psi})\eta_2 + (2\bar{k}_3 + \bar{k}_2\cos\bar{\Psi})\eta_3 - (\bar{k}_2\bar{k}_3\sin\bar{\Psi})\eta_5\Big] \quad \text{(T4:1)}$$

$$\varepsilon_2 = (m_a/\dot{\bar{\phi}}_2)\Big[(2b)^{\frac{1}{2}}(2\bar{k}_2 + \bar{k}_3\cos\bar{\Psi})\eta_1 + (\bar{k}_2 - b\bar{k}_3\cos\bar{\Psi})\eta_2 + (2\bar{k}_3 + b\bar{k}_2\cos\bar{\Psi})\eta_3 - (b\bar{k}_2\bar{k}_3\sin\bar{\Psi})\eta_5\Big] \quad \text{(T4:2)}$$

$$\dot{\eta}_1 = -\left(\bar{k}_1/2\dot{\bar{\phi}}_1\right)\Big\{\hat{H}\,\varepsilon_1 + \dot{\varepsilon}_1 - 2m_a\Big[(\bar{k}_3\eta_2 + \bar{k}_2\eta_3)\sin\bar{\Psi} + \bar{k}_2\bar{k}_3\eta_5\cos\bar{\Psi}\Big]\Big\} \quad \text{(T4:3)}$$

$$\dot{\eta}_2 = -\left(\bar{k}_2/2\dot{\bar{\phi}}_2\right)\Big\{\hat{H}\,\varepsilon_2 + \dot{\varepsilon}_2 + 2m_a\Big[(2b)^{\frac{1}{2}}\bar{k}_3\eta_1 - b\bar{k}_3\eta_2 + b\bar{k}_2\eta_3\Big]\sin\bar{\Psi} + 2m_a b\bar{k}_2\bar{k}_3\eta_5\cos\bar{\Psi}\Big\} \quad \text{(T4:4)}$$

$$\ddot{\eta}_3 = -2m_a\Big[(2\bar{k}_3 + \bar{k}_2\cos\bar{\Psi})\bar{k}_1\eta_1 + (2\bar{k}_3 + b\bar{k}_2\cos\bar{\Psi})\bar{k}_2\eta_2\Big] - \hat{H}\,\dot{\eta}_3 + \Big[\dot{\phi}^2 - 1 - m_a\,(2\bar{k}_1^2 + 2\bar{k}_2^2 + 3\bar{k}_3^2)\Big]\eta_3 + 2\bar{k}_3\dot{\phi}\dot{\eta}_4 - (\sin\bar{\phi}_{30})\eta_4 + (2m_a b\bar{k}_2^3\sin\bar{\Psi})\eta_5 \quad \text{(T4:5)}$$

$$\bar{k}_3\,\ddot{\eta}_4 = -2m_a\bar{k}_2\sin\bar{\Psi}\,(\bar{k}_1\eta_1 + b\bar{k}_2\eta_2) - \dot{\phi}(2\dot{\eta}_3 + \hat{H}\eta_3) - \hat{H}\,\bar{k}_3\dot{\eta}_4 - (\cos\bar{\phi}_{30})\eta_4 - (2m_a b\bar{k}_2^3\cos\bar{\Psi})\eta_5 \quad \text{(T4:6)}$$

$$\dot{\eta}_5 = 2\varepsilon_1 - \varepsilon_2 - \dot{\eta}_4 \quad \text{(T4:7)}$$

The differential equations for η_3 and η_4, however, must be obtained from Equation (3). In our previous use of Equation (3), the phase and amplitude of the one- and two-modes were allowed to be functions of the independent variable in the assumed quasi-linear solution, Equation (4), but k_3 and ϕ_{30} were required to be constant.

In order to derive the proper equations for η_3 and η_4, our assumed quasi-linear solution, Equation (4), must be enlarged to include these variables:

$$\tilde{\xi} = \delta_{T0}\left[k_1 e^{i\phi_1} + k_2 e^{i\phi_2} + (\bar{k}_3 + \eta_3)e^{i(\phi + \bar{\phi}_{30} + \eta_4)}\right] \quad (55)$$

Equation (55) is now substituted in Equation (3); the result is divided by $\exp i(\phi + \bar{\phi}_{30} + \eta_4)$ and averaged over a distance that is large compared to the various wavelengths involved.[2] The real and imaginary parts of the resulting equations are the differential equations in η_3 and η_4 given in Table 4 .

The usual procedure for stability analyses is to assume solutions to the perturbation equations of the form

$$\eta_j = \eta_{j0}\, e^{\lambda\tau}, \qquad j = 1, 2 \ldots N \quad (56)$$

where N, the number of parameters, is in our case five. Equation (56) is then substituted in the N perturbation equations; the result is a system of N homogeneous linear equations in the η_{j0}'s, with coefficients involving λ . Let DET be the N-th order determinant of this system. If M is the sum of the orders of the N perturbation equations (M = 7 for the equations of Table 4), the equation DET = 0 yields an M-th order polynomial equation in λ, the characteristic equation of the system:

$$a_0\lambda^M + a_1\lambda^{M-1} + \ldots + a_{M-1}\lambda + a_M = 0 \quad (57)$$

where the a_1's are assumed real. Let $r_1, r_2 \ldots r_M$ be the roots of this equation. Then the system represented by Equation (57) is

1. <u>stable</u> if the real parts of the M roots are all negative:

$$R\{r_k\} < 0, \quad k = 1, 2, \ldots M \quad (58)$$

2. critically stable if (57) has one or more non-repeated pure imaginary roots (including the root 0 i), but the remaining roots have negative real parts;

3. unstable if (57) has either

a. one or more roots with positive real part

or

b. repeated pure imaginary roots.

Note from 2 and 3 above that if the characteristic equation (57) has one zero root, the system will be either critically stable or unstable, but if (57) has more than one zero root, the system can only be unstable.

It is not necessary to evaluate the roots to test for stability: most stability tests are made directly on the coefficients a_i . For zero damping (see the next section), fairly elementary tests suffice; for nonzero damping (see the final section), we will require the more sophisticated Routh-Hurwitz stability criterion.

VII. STABILITY FOR ZERO DAMPING

Numerical integrations of Equation (3) led us to suspect that the zero-damping point $(0, \pi)$ in Figure 6 and Table 3 represents unstable solutions. To prove this, we set $\hat{H} = 0$ (and hence $\sin\bar{\phi}_{30} = \sin\bar{\Psi} = 0$) in the perturbation equations of Table 4 and make the simplifying assumptions listed in Table 5. The resulting approximate perturbation equations (T5:1-7) are also listed in Table 5.

Substituting the assumed solution (56) in Equations (T5:1-7), we obtain the characteristic equation:

$$\lambda^7 + a_2\lambda^5 + a_4\lambda^3 + a_6\lambda = 0 \qquad (59)$$

When a_2, a_4 and a_6 have been simplified (by the same assumptions made in Table 5 and by the use of Equation (T1:4) with $b = 1$, $\bar{k}_3^2 = 0$), we obtain:

$$a_2 \cong 2(1 + \dot{\phi}^2 + 6m_a\bar{k}_2^2)$$

$$a_4 \cong (1 - \dot{\phi}^2 + 6m_a\bar{k}_2^2)^2 + 72(m_a\bar{k}_2^2)^2 - 117m_a{}^2\bar{k}_2^3\left[(1 + 3\dot{\phi}^2)\bar{k}_3 + \cos\bar{\phi}_{30}\right]\cos\bar{\Psi}/\dot{\phi}^2$$

$$a_6 \cong 9m_a{}^2\bar{k}_2^3\left[13(\dot{\phi}^2 - 1) - 60m_a\bar{k}_2^2\right]\cos\bar{\phi}_{30}\cos\bar{\Psi}/\dot{\phi}^2$$

TABLE 5. APPROXIMATE PERTURBATION EQUATIONS FOR $I_x/I_y << 1$ AND $\hat{H} = 0$

ASSUMPTIONS:

$$b = 1$$

$$\bar{k}_3 << \max(1, \bar{k}_2)$$

$$k_j \dot{\epsilon}_j << \dot{\eta}_j \qquad j = 1, 2$$

$$\dot{\bar{\phi}}_1 = -\dot{\bar{\phi}}_2 = \dot{\phi}/3$$

EQUATIONS:

$$\epsilon_1 = (3m_a \bar{k}_2/\dot{\phi})\left[\sqrt{2}\,\eta_1 + 2\,\eta_2 + (\cos\bar{\Psi})\eta_3\right] \qquad \text{(T5:1)}$$

$$\epsilon_2 = -(3m_a \bar{k}_2/\dot{\phi})\left[2\sqrt{2}\,\eta_1 + \eta_2 + (\cos\bar{\Psi})\eta_3\right] \qquad \text{(T5:2)}$$

$$\dot{\eta}_1 = \sqrt{2}\,(3m_a \bar{k}_2^2 \bar{k}_3 \cos\bar{\Psi}/\dot{\phi})\eta_5 \qquad \text{(T5:3)}$$

$$\dot{\eta}_2 = (3m_a \bar{k}_2^2 \bar{k}_3 \cos\bar{\Psi}/\dot{\phi})\eta_5 \qquad \text{(T5:4)}$$

$$\ddot{\eta}_3 = -2m_a \bar{k}_2^2 \cos\bar{\Psi}(\sqrt{2}\,\eta_1 + \eta_2) + (\dot{\phi}^2 - 1 - 6m_a \bar{k}_2^2)\eta_3 + 2\bar{k}_3 \dot{\phi}\dot{\eta}_4 \qquad \text{(T5:5)}$$

$$\bar{k}_3 \ddot{\eta}_4 = -2\dot{\phi}\dot{\eta}_3 - (\cos\bar{\phi}_{30})\eta_4 - (2m_a \bar{k}_2^3 \cos\bar{\Psi})\eta_5 \qquad \text{(T5:6)}$$

$$\dot{\eta}_5 = (3m_a \bar{k}_2/\dot{\phi})\left[4\sqrt{2}\,\eta_1 + 5\,\eta_2 + (3\cos\bar{\Psi})\eta_3\right] - \dot{\eta}_4 \qquad \text{(T5:7)}$$

where $\cos\bar{\phi}_{30} = \pm 1$

$\cos\bar{\Psi} = \pm 1$

or, using Approximation (32) and assuming $\dot{\phi} > 2.5$,

$$a_2 \cong (23/10)\dot{\phi}^2 \tag{60a}$$

$$a_4 \cong (17/20)^2\dot{\phi}^4 \tag{60b}$$

$$a_6 \cong (207/80)(\dot{\phi}^2 - 9)m_a\bar{k}_2\cos\bar{\phi}_{30}\cos\bar{\Psi} \tag{60c}$$

Equation (59) has at least one zero root; hence the system is either critically stable or unstable. Removing this root from (59), we obtain the sixth order equation

$$(\lambda^2)^3 + a_2(\lambda^2)^2 + a_4(\lambda^2) + a_6 = 0 \tag{61}$$

The three roots (s_1, s_2, s_3) of this cubic in λ^2 yield the remaining six roots of Equation (59):

$$\lambda = 0, \pm\sqrt{s_1}, \pm\sqrt{s_2}, \pm\sqrt{s_3}$$

For critical stability, s_1, s_2 and s_3 must be real, negative and unequal:

1. real and negative so that the six square roots are pure imaginaries; otherwise $+\sqrt{s_i}$ or $-\sqrt{s_i}$ would have a positive real component;

2. unequal because repeated pure imaginary roots indicate instability.

The requirement that s_1, s_2 and s_3 be real and unequal is satisfied if the discriminant of Equation (61) is negative:

$$Q^3 + R^2 < 0 \tag{62}$$

where

$$Q = \frac{3a_4 - a_2^2}{9}$$

$$R = \frac{9a_2a_4 - 27a_6 - 2a_2^3}{54}$$

Substituting our approximations for a_2, a_4 and a_6, we have

$$Q \cong -\frac{1249}{3600}\dot{\phi}^4 \cong -0.347\dot{\phi}^4$$

$$R \cong -\frac{37513}{216000}\dot{\phi}^6 \cong -0.174\dot{\phi}^6$$

Hence Inequality (62) is always satisfied:

$$Q^3 + R^2 \cong -0.0116\dot{\phi}^{12} < 0$$

and the three roots are real and unequal.

To determine when the three roots are negative, we use the Descartes Rule of Signs: the number of positive real roots of the cubic (61) is equal to (or two less than) the number of sign changes in the sequence $1, a_2, a_4, a_6$. Since a_2 and a_4 are positive, there will be no sign changes and hence no positive real roots if and only if

$$a_6 > 0 \tag{63}$$

Since we have already shown that all three roots are real, Inequality (63) is the condition for three negative roots.

To summarize: for zero damping, critical stability requires that s_1, s_2 and s_3 be real, negative and unequal; the three roots are always real and unequal; they are negative if and only if condition (63) holds.

Now consider our expression for a_6, Equation (60c). Since $(\dot{\phi}^2 - 9)m_a$ is always positive and since $\cos\bar{\phi}_{30} = \pm 1$, $\cos\bar{\Psi} = \pm 1$ for zero damping, condition (63) reduces to

$$\cos\bar{\phi}_{30}\cos\bar{\Psi} = 1 \tag{64}$$

That is, for zero damping, our system is critically stable when (64) holds and is unstable when the product of the cosines is -1.

This proves our conjecture on the instability of the point $(0, \pi)$ and justifies the labeling of the other points in Table 3 as stable or unstable. We can now turn to the stability analysis for nonzero damping with some confidence in our approach.

VIII. STABILITY FOR NONZERO DAMPING

For nonzero damping, the assumed solutions (56) were substituted in the perturbation equations of Table 4. None of the assumptions and approximations that simplified our zero-damping analysis were applied to the nonzero-damping equations. As a result, the coefficients of the seventh-order characteristic equation:

$$\lambda^7 + a_1\lambda^6 + a_2\lambda^5 + a_3\lambda^4 + a_4\lambda^3 + a_5\lambda^2 + a_6\lambda + a_7 = 0 \qquad (65)$$

were truly horrendous functions of m_a, $\dot{\phi}$ and $\hat{H}$ (none of them vanishing everywhere as did a_1, a_3 and a_5 for zero damping). The opportunities for elementary algebraic blunders were many and we seemed to miss few of these opportunities. However, by a series of independent checks and double-checks we obtained what we managed to convince ourselves was an error-free set of expressions for the a_1's. To test these coefficients for stability, we used the Routh-Hurwitz criterion given in Table 6.

TABLE 6. ROUTH-HURWITZ STABILITY CRITERION

The real parts of the M roots of the equation

$$a_0\lambda^M + a_1\lambda^{M-1} + \ldots + a_{M-1}\lambda + a_M = 0 \qquad (T6:1)$$

will all be negative if and only if

$$T_i > 0 \ , \ i = 0, 1, 2, \ldots M \qquad (T6:2)$$

where

$$T_0 = a_0 \qquad (T6:3)$$

$$T_1 = a_1 \qquad (T6:4)$$

and T_n, $n \geq 2$, is the n-th order determinant of the upper left nxn elements of the array

$$\begin{array}{ccccccc} a_1 & a_0 & 0 & 0 & 0 & . & . \\ a_3 & a_2 & a_1 & a_0 & 0 & . & . \\ a_5 & a_4 & a_3 & a_2 & a_1 & . & . \\ a_7 & a_6 & a_5 & a_4 & a_3 & . & . \\ . & . & . & . & . & & \\ . & . & . & . & . & & \end{array} \qquad (T6:5)$$

Our complete procedure was as follows. For a given m_a and $\dot{\phi}$:

1. We assigned a value to any one of the trio $\hat{H}$, $\bar{\phi}_{30}$, $\bar{\Psi}$ and solved (by an iterative process) the equations of Table 1 for the remaining parameters. That is, we obtained a solution point

$$\bar{A} = (\bar{k}_1, \bar{k}_2, \bar{k}_3, \bar{\phi}_{30}, \bar{\Psi})$$

for a specified m_a and $\dot{\phi}$ and a specified or determined $\hat{H}$. (The option to evaluate results at a specified $\bar{\phi}_{30}$ or $\bar{\Psi}$, rather than at a specified $\hat{H}$, proved useful: in certain regions of the $\bar{\Psi}$, $\bar{\phi}_{30}$ plane, the convergence of the iterative process was improved by fixing one or the other of the two angles.)

2. At point $\bar{A}$ we evaluated the coefficients a_i of the characteristic equation (65) formed from the perturbation equations of Table 4.

3. Finally, we evaluated the Routh-Hurwitz determinants of Table 6 to test point $\bar{A}$ for stability.

The above process was incorporated into a single computer program and applied to hundreds of input values so that we could map out the stability regions in the solution plane and define the stability/instability boundary numerically.

For a given m_a and $\dot{\phi}$ and for any $\hat{H}$ less than $\hat{H}_{MAX}$, two solutions were obtained: one stable and one unstable. In every case, the boundary occurred (within the accuracy of the computations) at a point where $\hat{H} = \hat{H}_{MAX}$. This was precisely our conjecture.

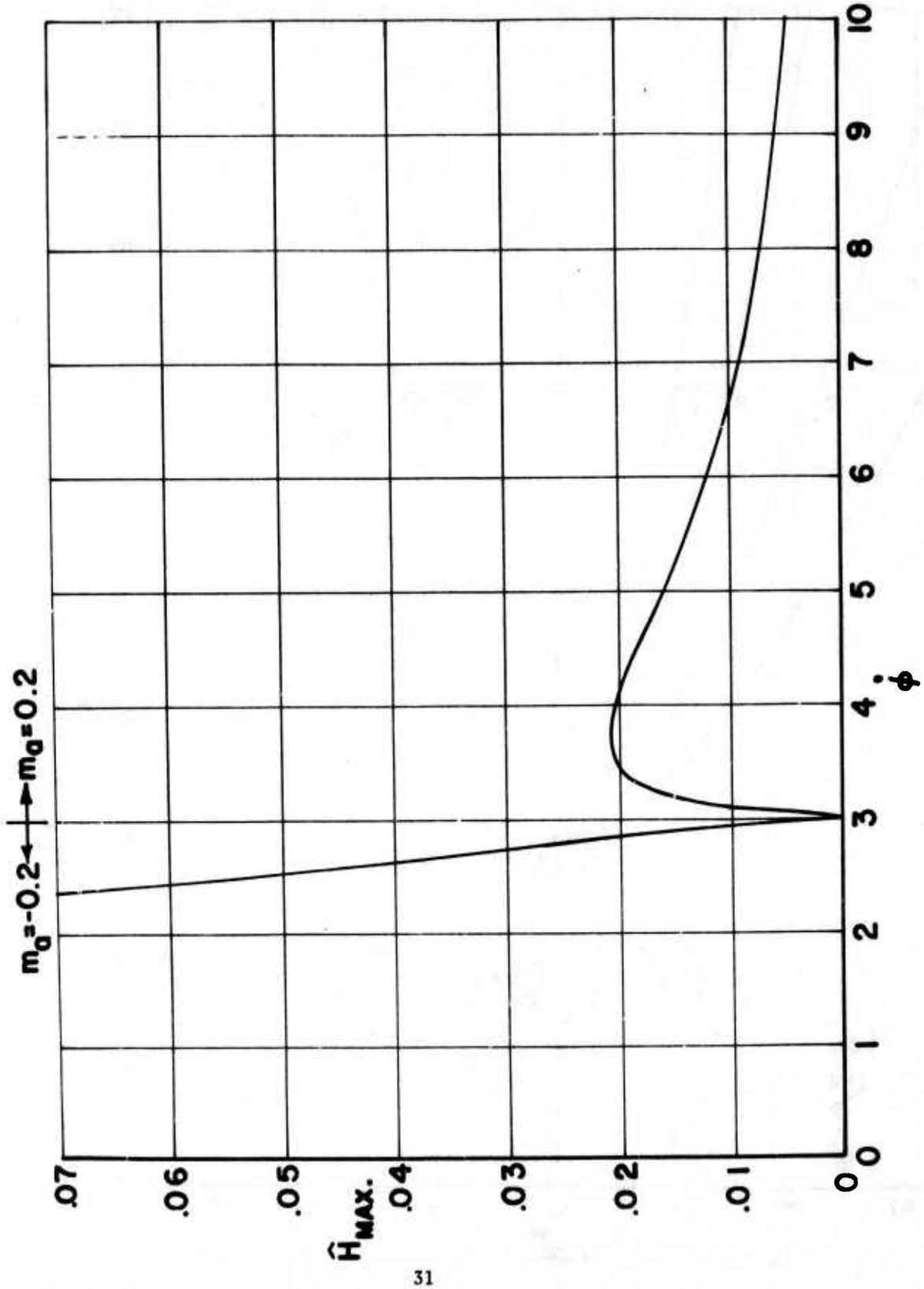

Figure 1. $\hat{H}_{MAX}$ versus $\dot{\phi}$ ($m_a = \pm 0.2$)

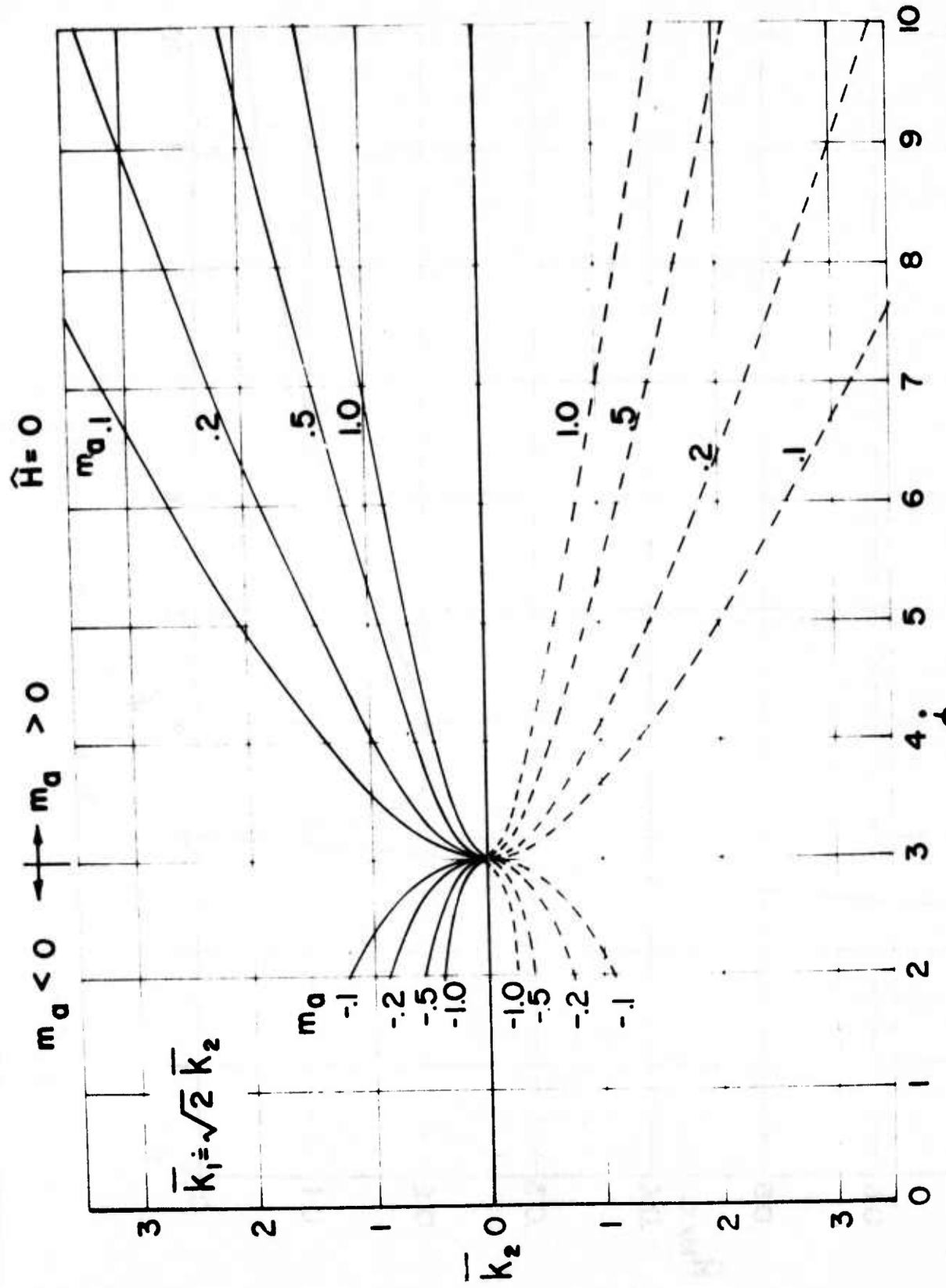

Figure 2. $\bar{k}_2$ versus $\dot{\phi}$ ($\hat{H} = 0$, various m_a)

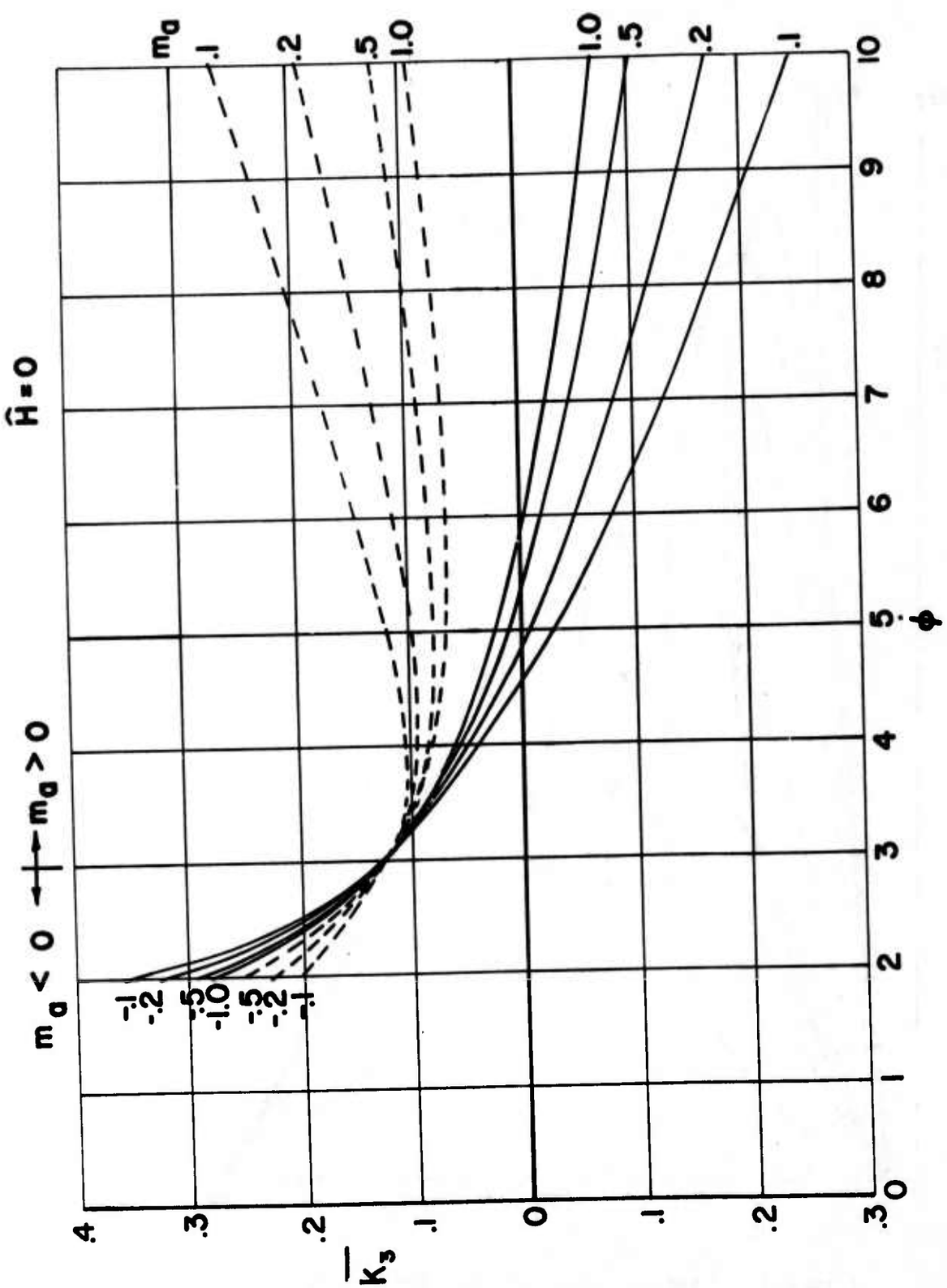

Figure 3. $\bar{k}_3$ versus ϕ ($\hat{H} = 0$, various m_a)

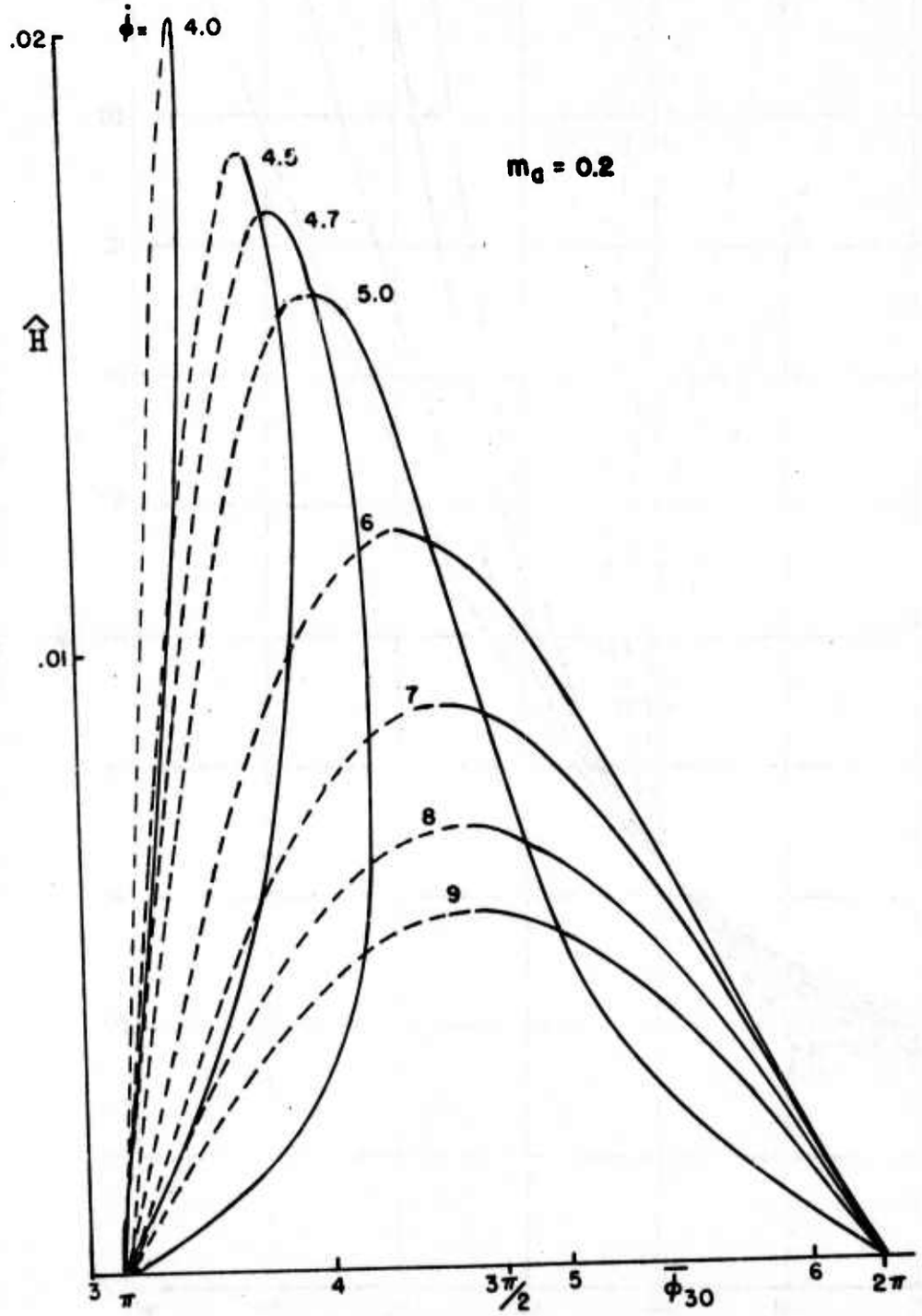

Figure 4. $\hat{H}$ versus $\bar{\phi}_{30}$ (m_a = 0.2, various $\dot{\phi}$)

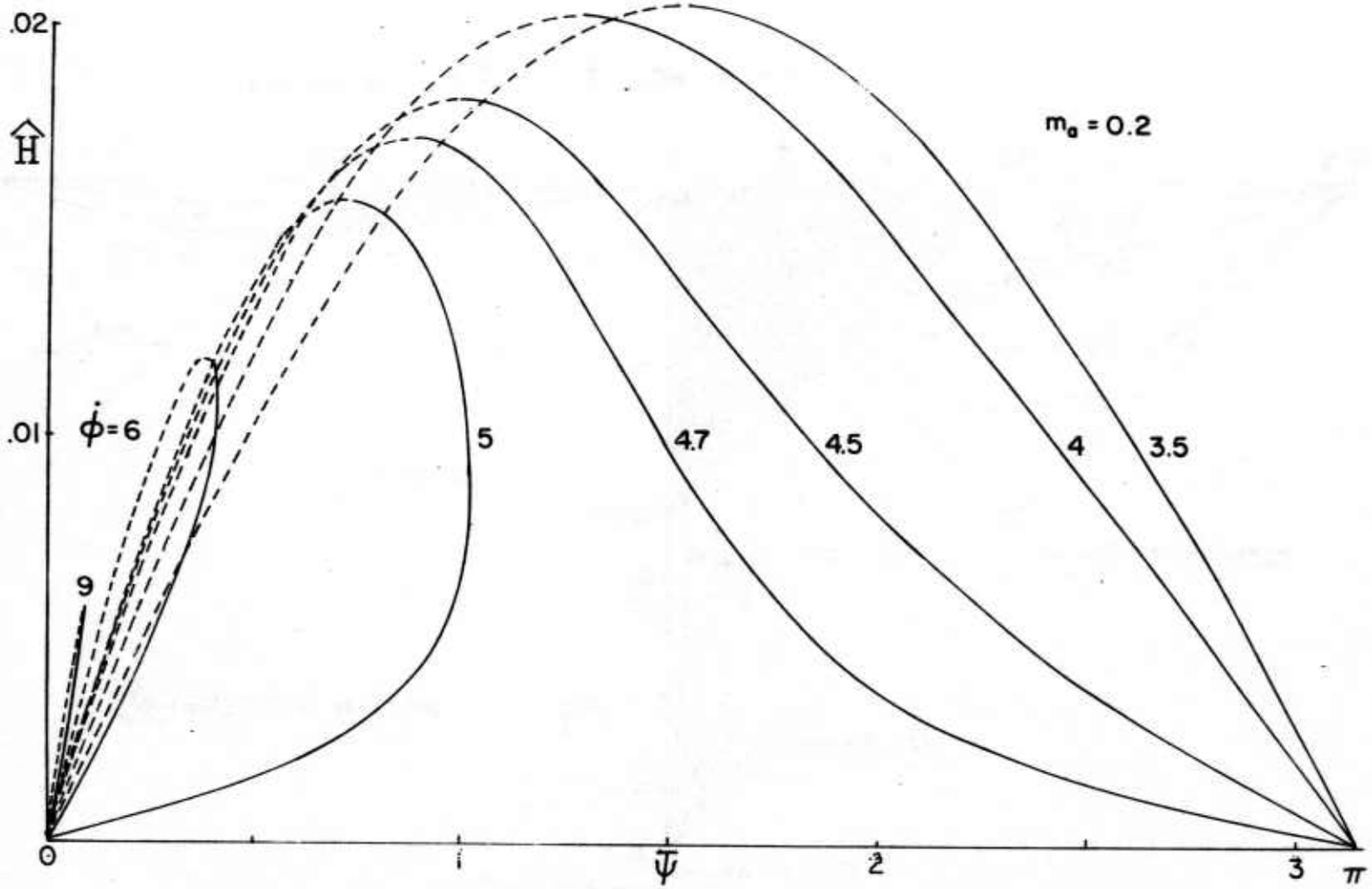

Figure 5. $\hat{H}$ versus $\bar{\Psi}$ (m_a = 0.2, various $\dot{\phi}$)

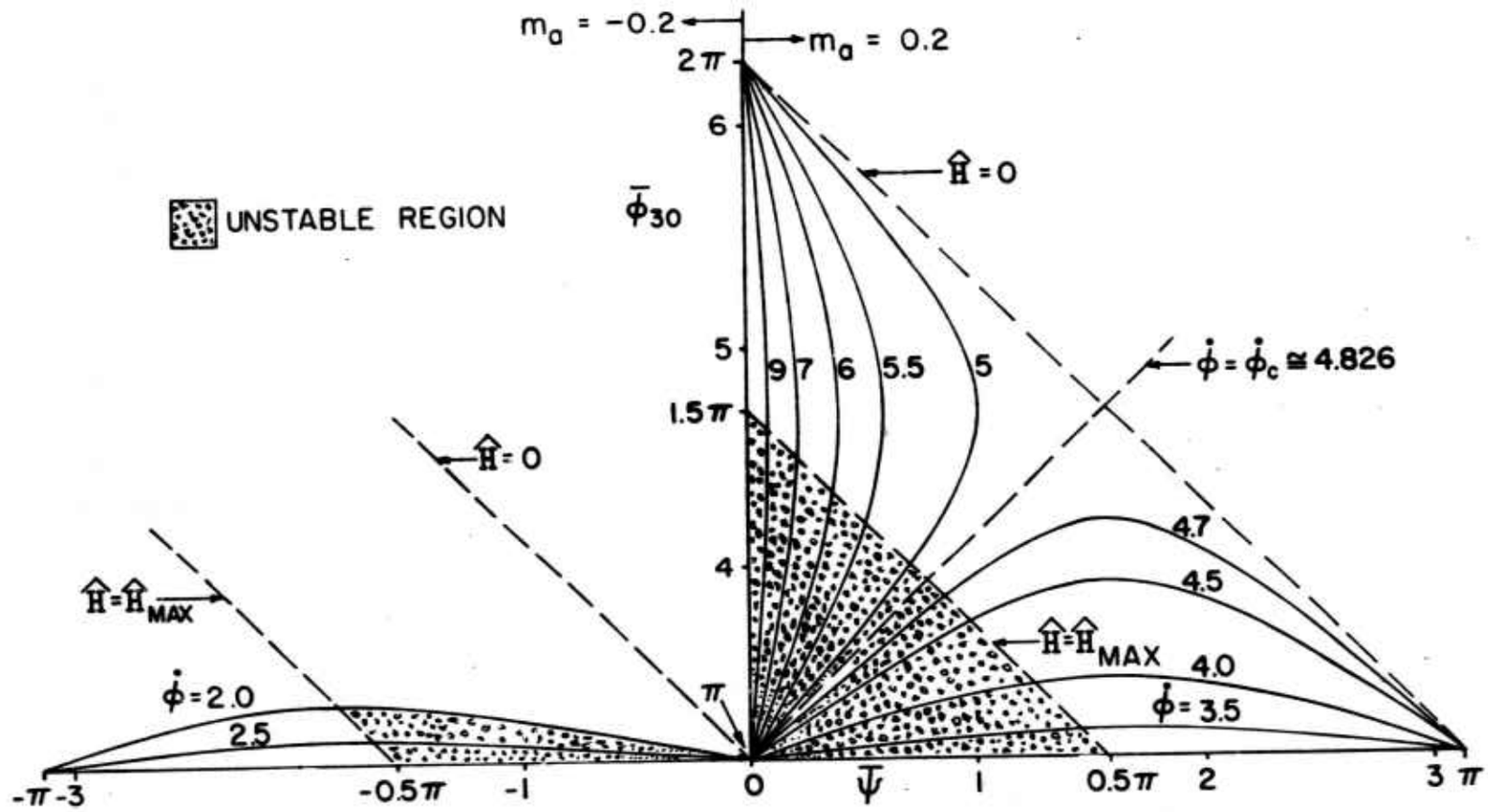

FIGURE 6 $\bar{\phi}_{30}$ VS $\bar{\psi}$ FOR $m_a = \pm 0.2$

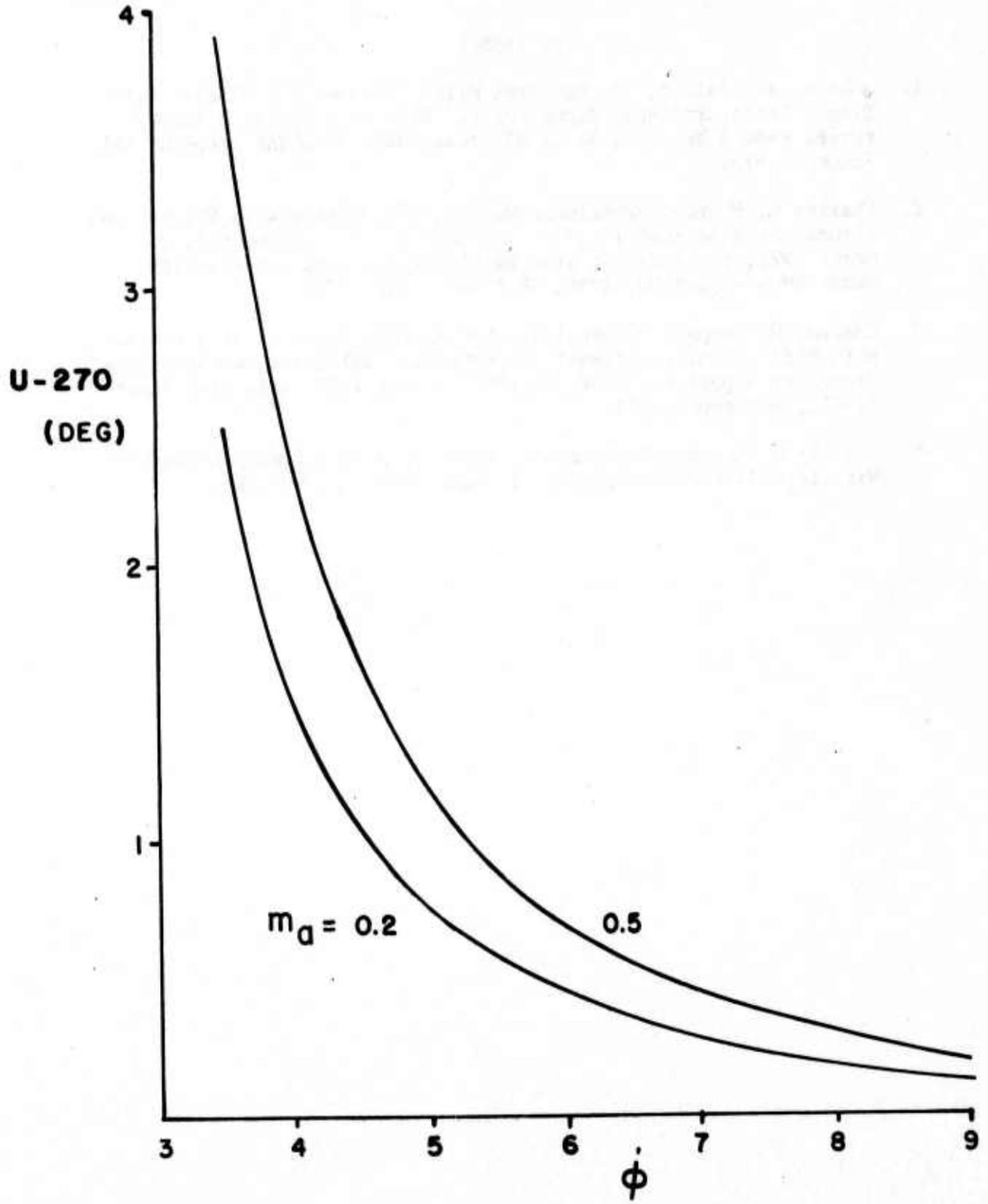

Figure 7. (U - 270°) versus $\dot{\phi}$ (m_a = 0.2, 0.5)

REFERENCES

1. John D. Nicolaides, "On the Free Flight Motion of a Missile with Slight Configurational Asymmetries," Ballistic Research Laboratories Report No. 858, AD 26405, June 1953; also IAS Preprint 395, January 1953.

2. Charles H. Murphy, "Nonlinear Motion of a Missile with Slight Configurational Asymmetries," *J. Spacecraft and Rockets*, Vol. 8, March 1971, pp. 259-263; also Ballistic Research Laboratories Memorandum Report No. 2036, AD 870704, May 1970.

3. Charles H. Murphy, "Generalized Subharmonic Response of a Missile with Slight Configurational Asymmetries," Ballistic Research Laboratories Report No. 1591, AD 749787, June 1972; also AIAA Paper 72-972, September 1972.

4. Charles H. Murphy, "Subharmonic Behavior of a Slightly Asymmetric Missile," *AIAA Journal*, Vol. 11, June 1973, pp. 884-885.

LIST OF SYMBOLS

$\bar{A}$	nonharmonic steady-state solution set $(\bar{k}_1, \bar{k}_2, \bar{k}_3, \bar{\phi}_{30}, \bar{\Psi})$
a_i	coefficient of λ^{M-i} in the characteristic equation (57)
b	$-\frac{2\bar{\dot{\phi}}_2}{\bar{\dot{\phi}}_1}$
b_M	maximum b (~ 1.14), the only positive root of the equation $D = 0$
$C_{\tilde{m}}, C_{\tilde{n}}$	transverse aerodynamic moment coefficients
C_{M_0}	aerodynamic moment coefficient due to asymmetry
C_{M_α}	static moment coefficient
$C_{M_q}, C_{M_{\dot{\alpha}}}$	damping moment coefficients
c_0, c_2	coefficients in a cubic static moment expansion: $C_{M_\alpha} = c_0 + c_2\delta^2$
D	$1 + 4b - 2b^2(1+b)$
F, f, f_1, f_2	functions
DET	determinant
H	$-\frac{\rho S \ell^3}{2I_y}\left(C_{M_q} + C_{M_{\dot{\alpha}}}\right)$
$\hat{H}_A$	damping factor approximation, Equation (40)
I_x, I_y	axial, transverse moments of inertia
k_1, k_2, k_3	magnitudes of the three modal arms, Equation (4)

LIST OF SYMBOLS (continued)

L_A	the locus of solution points at which $\bar{\phi}_{30} + \bar{\Psi} = 3\pi/2$; approximately L_H
L_H	the locus of solution points at which $\hat{H} = \hat{H}_{MAX}$; the conjectured stability/instability boundary
ℓ	reference length
m_a	$\dfrac{c_2 \delta_{T0}^2}{c_0} = \dfrac{C_{M_\alpha}\Big\vert_{\dot{\phi} = 0}}{C_{M_\alpha}\Big\vert_{\delta^2 = 0}} - 1$
M	order of the characteristic equation (57); sum of the orders of the perturbation equations
M_0	$\dfrac{\rho S \ell^3}{2 I_y} c_0$
N	number of parameters
P	$\dfrac{I_x}{I_y} \dfrac{p\ell}{V}$, the gyroscopic spin
$p, \tilde{q}, \tilde{r}$	X, $\tilde{Y}$, $\tilde{Z}$ components of the missile's angular velocity
Q, R	components of the cubic discriminant, Equation (62)
r_k	k-th root of the characteristic equation (57)
S	reference area
s	arclength along trajectory, in calibers
s_1, s_2, s_3	roots of the cubic equation (61)
T_i	i-th Routh-Hurwitz determinant, Table 6
U	the value of $(\bar{\phi}_{30} + \bar{\Psi})$ at $\hat{H} = \hat{H}_{MAX}$ for a given $\dot{\phi}$ and m_a

LIST OF SYMBOLS (continued)

$\tilde{v}$, $\tilde{w}$	$\tilde{Y}$, $\tilde{Z}$ components of the velocity
V	magnitude of the velocity
X, $\tilde{Y}$, $\tilde{Z}$	nonrolling Cartesian coordinate axes. The X-axis lies along the missile's axes of symmetry and the $\tilde{Y}$ and $\tilde{Z}$ axes are so constrained that (i) the $\tilde{Y}$-axis is initially in the horizontal plane and (ii) the angular velocity of the coordinate system has a zero X-component.
δ	$\lvert\tilde{\xi}\rvert$, the sine of the total angle of attack
δ_{TR}	trim angle at resonance
δ_{T0}	trim angle at zero spin
ϵ_1 , ϵ_2	perturbation in $\bar{\phi}_1$, $\bar{\phi}_2$
η_{j0}	value of η_j at $\tau = 0$, Equation (56)
η_1, η_2, η_3, η_4, η_5	perturbation in $\bar{k}_1$, $\bar{k}_2$, $\bar{k}_3$, $\bar{\phi}_{30}$, $\bar{\Psi}$
λ	damping factor in the assumed solution, Equation (30), to the perturbation equations
$\tilde{\mu}$	$\frac{(\tilde{q} + i\tilde{r})\ell}{V}$
$\tilde{\xi}$	$\frac{\tilde{v} + i\tilde{w}}{V}$
ρ	air density
τ	$(-M_0)^{\frac{1}{2}}$ s
ϕ	roll angle
$\dot{\phi}$	spin = roll rate = p
$\dot{\phi}_c$	critical spin; for a given m_a, the $\dot{\phi}$ value at $\bar{k}_3 = 0$

LIST OF SYMBOLS (continued)

ϕ_1 , ϕ_2	1- and 2-mode phase angles, Equation (4)
ϕ_{30}	initial value of the trim mode phase angle, Equation (4)
Ψ	$2\phi_1 - \phi_2 - \phi - \phi_{30}$, Equation (8)

Superscripts

$( )'$	$d( )/ds$
$(\dot{})$	$d( )/d\tau$
$(\hat{})$	$( ) \quad (-M_0)^{-\frac{1}{2}}$
$(\bar{})$	value associated with some nonharmonic steady-state motion
$(\tilde{})$	value in the nonrolling coordinate system

Subscripts

$( )_{av}$	average over a distance that is large compared with the wavelengths involved
$( )_{MAX}$	maximum value for a given $\dot{\phi}$ and m_a

DISTRIBUTION LIST

No. of Copies	Organization
2	Commander Defense Documentation Center ATTN: DDC-TCA Cameron Station Alexandria, Virginia 22314
2	Commander U.S. Army Materiel Command ATTN: AMCDMA, Mr. N. Klein Mr. J. Bender 5001 Eisenhower Avenue Alexandria, Virginia 22333
1	Commander U.S. Army Materiel Command ATTN: AMCRD, BG H.A. Griffith 5001 Eisenhower Avenue Alexandria, Virginia 22333
1	Commander U.S. Army Materiel Command ATTN: AMCRD-T 5001 Eisenhower Avenue Alexandria, Virginia 22333
1	Commander U.S. Army Aviation Systems Command ATTN: AMSAV-E 12th and Spruce Streets St. Louis, Missouri 63166
1	Director U.S. Army Air Mobility Research and Development Laboratory Ames Research Center Moffett Field, California 94035
1	Commander U.S. Army Electronics Command ATTN: AMSEL-RD Fort Monmouth, New Jersey 07703
1	Commander U.S. Army Missile Command ATTN: AMSMI-R Redstone Arsenal, Alabama 35809
1	Commander U.S. Army Tank Automotive Command ATTN: AMSTA-RHFL Warren, Michigan 48090
2	Commander U.S. Army Mobility Equipment Research and Development Center ATTN: Tech Docu Cen, Bldg. 315 AMSME-RZT Fort Belvoir, Virginia 22060
1	Commander U.S. Army Armament Command Rock Island, Illinois 61202
1	Commander U.S. Army Picatinny Arsenal ATTN: SARPA-FR-S, Mr. A. Loeb Dover, New Jersey 07801
1	Commander U.S. Army Harry Diamond Laboratories ATTN: AMXDO-TI 2800 Powder Mill Road Adelphi, Maryland 20783
1	Commander U.S. Army Materials and Mechanics Research Center ATTN: AMXMR-ATL Watertown, Massachusetts 02172

DISTRIBUTION LIST (continued)

No. of Copies	Organization
1	Commander U.S. Army Research Office ATTN: CRD-AA-EA P. O. Box 12211 Research Triangle Park North Carolina 27709
3	Commander U.S. Naval Air Systems Command ATTN: AIR-604 Washington, D.C. 20360
3	Commander U.S. Naval Ordnance Systems Command ATTN: ORD-0632 ORD-035 ORD-5524 Washington, D.C. 20360
1	Commander U.S. Naval Air Development Center, Johnsville Warminster, Pennsylvania 18974
1	Commander U.S. Naval Ship Research and Development Center ATTN: Aerodynamics Laboratory Washington, D.C. 20007
3	Commander U.S. Naval Weapons Center ATTN: Code 753 Code 4063 Code 607, Dr. W.R. Haseltine China Lake, California 93555
1	Commander U.S. Naval Surface Weapons Center ATTN: Tech Lib, Code 730 Silver Spring, Maryland 20910
1	Commander U.S. Naval Surface Weapons Center ATTN: Code K-1, Dr. Cohen Dahlgren, Virginia 22448
1	Superintendent U.S. Naval Postgraduate School Monterey, California 93940
1	AEDC (AEGT) Arnold AFS Tennessee 37389
1	ADTC (ADBRL-2) Eglin AFB Florida 32542
1	AFATL (DLR) Eglin AFB Florida 32542
1	AFATL (DLRD) Eglin AFB Florida 32542
1	AFATL (DLRV) Eglin AFB Flordia 32542
1	Director NASA Scientific and Technical Information Facility ATTN: SAK/DL Post Office Box 33 College Park, Maryland 20740
1	Director NASA George C. Marshall Space Flight Center ATTN: MS-I, Library Huntsville, Alabama 35812

DISTRIBUTION LIST (continued)

No. of Copies	Organization
1	Director NASA Langley Research Center ATTN: MS 185, Technical Lib Langley Station Hampton, Virginia 23365
1	Director NASA Lewis Research Center ATTN: Technical Library 21000 Brookpark Road Cleveland, Ohio 44135
1	Director Jet Propulsion Laboratory ATTN: Technical Library 4800 Oak Grove Drive Pasadena, California 91103
1	Calspan Corporation ATTN: J. Desmond Post Office Box 235 Buffalo, New York 14221
1	General Motors Corporation Defense Research Laboratories ATTN: Library Santa Barbara, California 93108
1	IIT Research Institute ATTN: Library 10 West 35th Street Chicago, Illinois 60616
1	Director Applied Physics Laboratory The Johns Hopkins University 8621 Georgia Avenue Silver Spring, Maryland 20910
1	Stanford University ATTN: Department of Aero- nautical Engineering Stanford, California 94305
1	University of California ATTN: Professor E.V. Laitone Berkeley, California 94704
1	University of Notre Dame Department of Mechanical Engineering ATTN: Dr. J.D. Nicolaides Notre Dame, Indiana 46556
1	University of Illinois Department of Aeronautical Engineering ATTN: Professor A.I. Ormsbee Urbana, Illinois 61801
	Aberdeen Proving Ground
	Marine Corps Ln Ofc Dir, USAMSAA